

COB-2023-0350

COMPARISON OF IMPACT RESISTANCE OF ANNEALED 3D PRINTED PLA ACCORDING TO DIFFERENT PROCESS PARAMETERS AND IZOD ASTM STANDARDS

Felipe dos Anjos Rodrigues Campos

Lucas Melo Queiroz Barbosa

Kauã Ferreira de Almeida

Pedro Henrique Veiga Oliveira

Thiago de Oliveira Santos

Leonardo Rosa Ribeiro da Silva

Federal University of Uberlândia, School of Mechanical Engineering, Av. João Naves de Ávila, 2121, Bloco 1M, 38400-902, Uberlândia, MG, Brazil

filipin_anjos@hotmail.com, lmqbarbosa@gmail.com, kau Almeida2013@hotmail.com, pedroh.veiga.o@gmail.com,

thiago.de@ufu.br, leinardo.rrs@gmail.com

Álison Rocha Machado

Graduate Program in Mechanical Engineering, Pontifícia Universidade Católica do Paraná – PUC-PR, R. Imaculada Conceição, 1155, Bairro Prado Velho, CEP 80215-901, Curitiba/PR, Brasil

alissonr.machado@gmail.com

Abstract. *The additive manufacture through the Fused Filament Fabrication (FFF) process is one of the most utilized techniques of 3D printing nowadays, which consists of the extrusion of a thermoplastic filament, provided. continuously from a spool, through a nozzle extruder heated for the material deposition in layers. In this process, the deposited polymer cools rapidly for the layer solidification, and then it is reheated with the deposition of the upper layers, making important the study of the thermoplastic properties in accord to the pieces thermal history, especially in relation to the glass transition temperature (T_g) and the crystallization temperature (T_c). The first indicates the temperature from which the polymeric chains gain mobility and relates with the adhesion between the deposited layers. The second marks the organization tendency of the macromolecules in crystals, that normally make the material more resistant, though less ductile. Due to this phenomenon, the FFF printed part's mechanical properties become dependent on parameters such as nozzle and table temperatures, and layer height, in addition to post-processing operations like annealing. In this sense, this research aimed to evaluate the influence of the printing parameters mentioned and annealing on the impact resistance of FFF fabricated polylactic acid (PLA) parts. It utilized a complete factorial type experimental planning with 2 levels and 4 variables (2^4), for 2 different types of specimens, that allowed use of variance analysis (ANOVA) to identify which are the most significant factors for the impact resistance evaluated according to the standards ASTM D4508 and ASTM D256. The annealing process was identified as the most influential parameter, since only 20 minutes reheating was enough to increase the piece's average resistance by more than 300% on average. The crystallinity change was discussed according to the change in the translucency of samples. The results demonstrated notable efficacy of the reheating process on improving the mechanical properties, pointing to a great cost-benefit strategy for the industrial segments and for professional consumers to improve their FFF printed parts.*

Keywords Additive manufacture, Annealing, Impact resistance, Crystallinity

1. INTRODUCTION

Currently, with the increased accessibility of modeling software and 3D printers, extrusion-based additive manufacturing has become increasingly popular in research. This is primarily due to its relatively low cost, quick production time, and high geometric accuracy of the produced parts. This technology is called Fused Filament Fabrication (FFF), a process that occurs when a thermoplastic filament is extruded through a nozzle and heated to the point of melting the polymer, which deposits the material in layers and shapes as indicated by a three-dimensional model digital, until reaching the desired result (Sood et al, 2010). There are several polymers that can be used for the realization of such printings, the most common being ABS and PLA.

Despite the advantages of the process, one of the main negative aspects of additive manufacturing by FFF is related to the porosity of the final solid, because as the part is manufactured by layers of filaments. The deposition process leaves a considerable amount of unfilled regions, and this factor contributes to a lower resistance of the final product. This phenomenon can be seen in Figure 1, where it is also evident the lack of contact between the layers deposited, preventing

intertwining between polymeric chains, which is the main mechanism of interfacial adhesion in printed pieces (Sun et al, 2008).

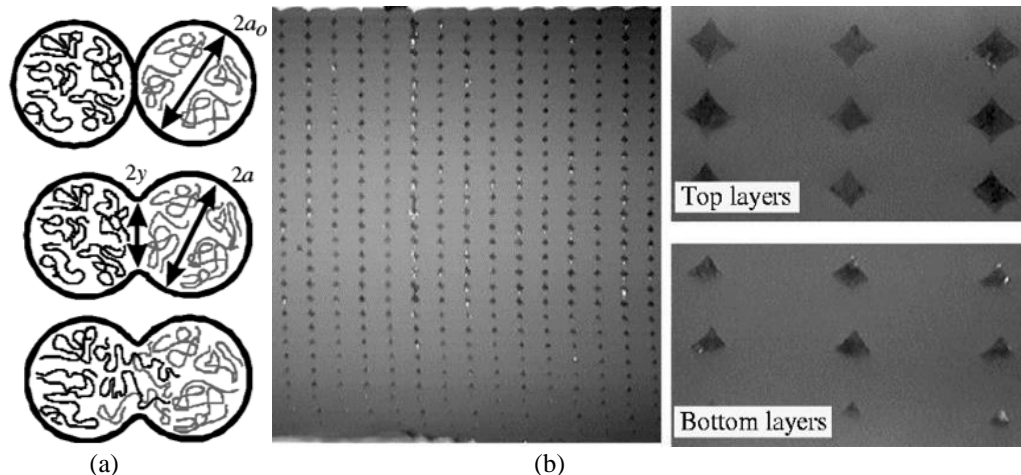


Figure 1. (a) Mechanism of sintering and molecular diffusion. (b) analysis of the interstices between the rows and layers, revealing greater adhesion at the bottom of the piece that spent more time above the vitreous transition temperature. Adapted from Sun et al (2008).

The resistance of the piece produced by FFF also depends directly on its thermal properties. After the material is extruded, it suffers a fast loss of thermal energy due to the contact with the other layers and the external air. During this period in which the material remains above its glass transition temperature (T_g), polymer chains have high rotational mobility and can either intertwine with the chains of adjacent layers (increasing adhesion) or crystallize, depending on the type of polymer (Hart et al, 2020). In the case of PLA, usually printed at around 200 °C and with a T_g close to 50 °C according to Vaes and Puyvelde (2021), the chains are initially disordered after exiting the nozzle, characterizing the amorphous state, and tend to crystallize as the temperature decreases. The rate of crystallization depends on the cooling rate and/or the time in which the polymer remains above its T_g , being influenced, therefore, by printing parameters such as table temperature, nozzle temperature and fan cooling power (Torres et al, 2016). That becomes important for the final characteristics because the level of crystallinity relates to the mechanical properties, chemical and thermal resistance, and the translucency of printed parts (Gao et al, 2021).

Considering this deficit in relation to the resistance of the samples, several studies seek to evaluate which parameters contribute more to improve this property. Many studies demonstrate that infill and wall thickness are beneficial for mechanical strength (Aliheidari et al, 2017). However, such printing criteria raise material and time costs significantly, so the cost of a part with these conditions would be less viable. At the same time, several works have also explored possibilities of optimization of thermal parameters to improve the resistance of the part, including the use of post-treatment by annealing (Bhandari et al, 2019). In these cases, researchers employ intricate analytical and computational models, together with fracture toughness analysis in high-cost equipment to explain the material behavior changes.

This work sought to address how thermal phenomena alter the properties of printed parts subject to high shear rate typical of impact loads, by performing simpler and faster experiments. Thus, using an experimental design of the full factorial type, the four variables nozzle temperature, table temperature, type of impact testing and the annealing process were evaluated in two levels to see how they alter the impact strength and translucency of the samples, with the last being used as a way of measuring the material crystallinity change due to annealing. For this, the Izod-type test was applied in the PLA samples, analyzing the energy absorbed in the fracture and the opacity of the samples. The statistical analysis of the data by ANOVA allowed the determination of which parameters are statistically significant for changes in the properties and provided an interesting alternative to study the behavior of printed materials.

2. METHODOLOGY

2.1 Preparations of the samples

The parts used in the impact tests were printed from natural polylactic acid (PLA) filaments, diameter 1.75 mm, of 3DFila brand. Test samples were produced by additive manufacturing using the method Fused Filament Fabrication (FFF) through a 3D printer Creality Ender 3 for different impact test methods, varying also the printing parameters (table temperature, T_{table} , and nozzle temperature, T_{nozzle}) and with or without annealing. This resulted in an experimental design of the complete factorial type in 2 levels and 4 variables (2^4), with sample parameters A to H, as shown in Table 1, being used for both Izod standards ASTM D256 (2018) and ASTM D4508 (2006). It should be noted that during printing, all other parameters remained constant, such as layer height (0.2 mm), printing speed (50 mm/s), nozzle size

(0.4 mm), among others. The choice of printing parameters considered the most suitable limits recommended by the filament manufacturer and previous results from other works (Almeida et al., 2023).

Table 1. Complete factorial experimental design 2³.

| Test condition | Ttable (°C) | Tnozzle (°C) | Annealing |
|----------------|-------------|--------------|-----------|
| A | 85 | 215 | without |
| B | 85 | 200 | without |
| C | 50 | 200 | without |
| D | 50 | 215 | without |
| E | 85 | 215 | with |
| F | 85 | 200 | with |
| G | 50 | 200 | with |
| H | 50 | 215 | with |

2.2 Annealing

The influence of post-treatment by annealing was studied by subjecting the parts to controlled heating in an electric oven. Half of the printed pieces were annealed in a 10 L electric furnace, Britânia brand, with 1050 W power and a timer that allows automatic shutdown. The samples were placed inside the equipment before its activation and annealed for 20 minutes in a temperature range of around 100 °C to 120 °C, as exemplified in the graph of Figure 2. The oven's internal temperature was measured using 4 thermocouples type K associated with MAX31855 modules connected to an Arduino Uno microcontroller with ATmega processor 328. The data was obtained using the Arduino as a signal acquisition board connected to a notebook, with data recording by CoolTerm 2.0 software. After completing the annealing process and turning off the oven, the parts were kept inside for 20 minutes for cooling before manipulation.

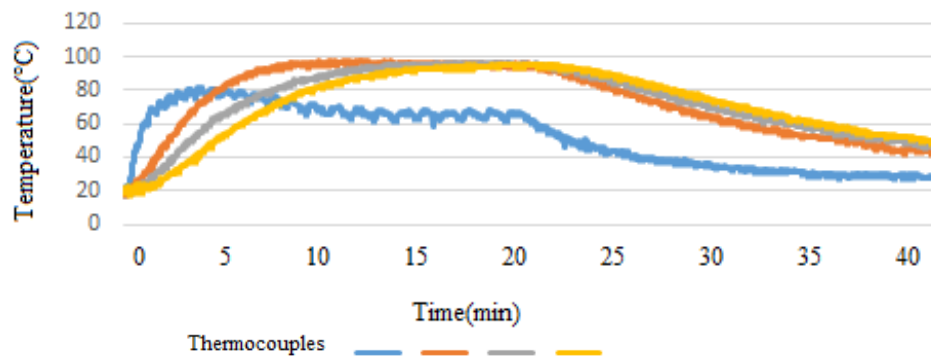


Figure 2. Graphic of the annealing and cooling temperature of the D256 samples by time

2.3 Impact test

The Izod-type impact tests were performed according to the ASTM D4508 and ASTM D256 standard in order to obtain the energy absorbed by the samples during its fracture, so as to evaluate the influence of thermal parameters on the resistance of parts at dynamic loads and compare them with one another. The pendulum used has a length of 0.778 m (distance from the pendulum tip to the center of rotation), with total mass of 0.992 kg and center of mass 0.378 m from the center of rotation. The pendulum was raised at a 90° inclination before release, being parallel to the horizontal base of the impact testing machine, resulting in a total energy of 3.68 J and an impact velocity of 5.6 m/s when hitting the sample. All tests followed these standards, and in the final calculation of the energy absorbed by the test specimens, it was discounted the portion of pendulum energy converted into kinetic energy of the fractured part of the sample, thrown after the impact of the pendulum, as recommended by the standards.

Using a pachymeter, measurements of the D256 samples were made, its width, lengths and thickness were taken three times on each specimen, this was then used to verify if the annealing process would cause any geometric changes in the samples, once this phenomenon is known to take place due to crystallization process (Lluch-Cerezo et al., 2022). Figure 3 shows the ideal dimensions of the specimens according to ASTM D256 and D4508 respectively.

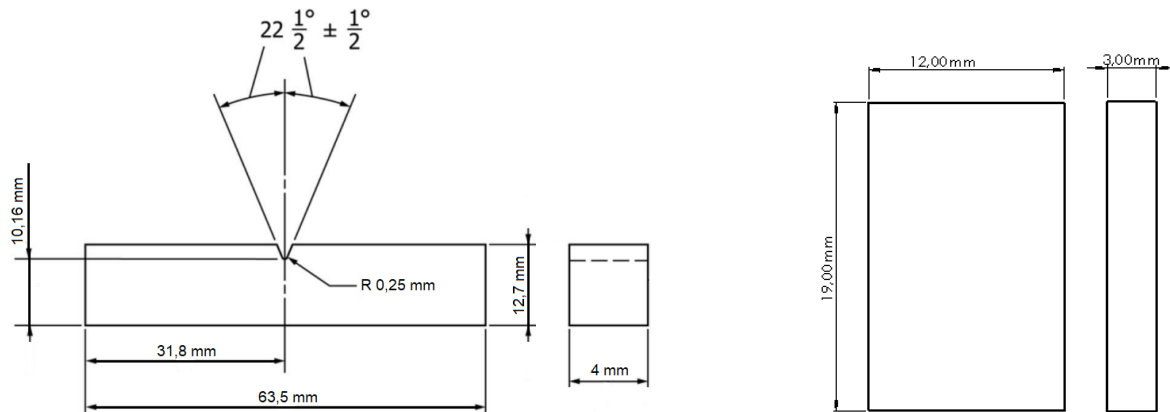


Figure 3. Example of specimens for Izod type test according to ASTM D256 (left) and D4508 (right).

The pendulum calibration was carried out by using a smartphone in the video recording function in slow motion mode, which can record 240 frames per second, analyzing the distance traveled by the tip of the pendulum between one frame and the other, with a rule behind the pendulum. Thus, it was possible to find the impact velocity of the pendulum in the sample, and the energy was calculated according to its dimensions, considering its rotational moment of inertia. The friction was also accounted by releasing the pendulum with no sample and checking how much energy was absorbed by air and bearing friction.

To capture data on the energy absorption of the pendulum by the sample, an encoder type sensor was used, to measure the maximum inclination reached by the pendulum. The encoder consists of a disk of diameter approximate 220 mm with 360 holes 1 mm wide and equally spaced by 1 mm at the edge of the disc, associated with an optical module in a manner similar to that shown in Figure 4a. The LM393 module used can be seen in Figure 4b, while assembly of the machine was done as exemplified in Figure 4c, with the encoder disk replacing the pointer scale. The sensor signal was also checked on an Arduino-type microcontroller, which was connected via USB cable to a mobile phone. The programming used informed the operator the angle displaced by the pendulum with a precision of 0.5°, making it possible to calculate the maximum height reached by the pendulum in comparison with the initial height in the moment of release.

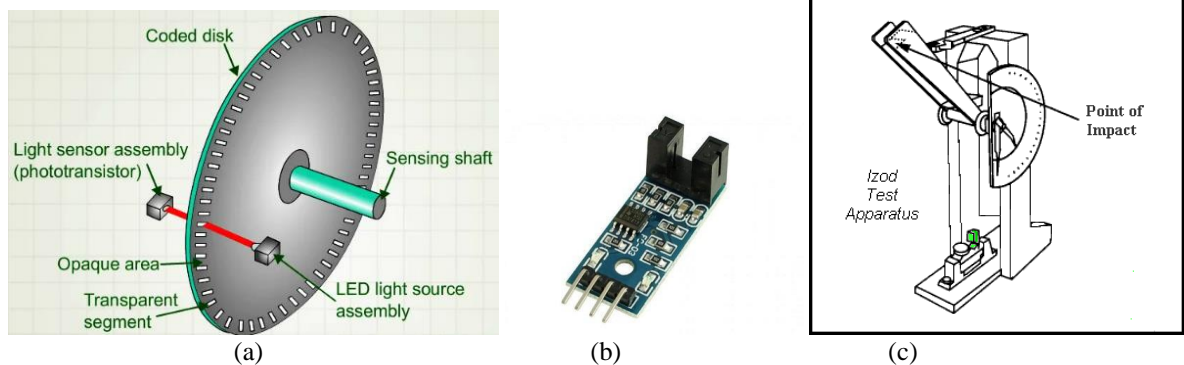


Figure 4. (a) Representative encoder-type sensor schematic (adapted from Instrumentation Tools, 2022). (b) Sensor LM393 optical compatible with Arduino used in the encoder. (c) Example of mounting the encoder on the test machine Izod-type impact (adapted from MatWeb, 2022).

2.4 Samples's opacity

The encoder's optical sensor was also used to measure the opacity of the evaluated samples, introducing the fractured piece manually between the LED and the photoreceptor. The passage of the light beam through the material changes the electronic signal provided by the module according to the sample's translucency. In the case of semicrystalline polymers such as PLA, the formation of crystals would generate more compact structures, which do not allow the passage of light between the polymeric chains. In this sense, this method can be used as a tool for estimating crystallinity, although the correct calculation of this property must be done through more reliable tests (Piorkowska and Rutledge, 2013), such as differential scanning calorimetry (also known as DSC, from Differential Scanning Calorimetry) and Dynamic Mechanical Analysis (DMA).

3. RESULTLS AND ANALYSIS

The samples impact strength can be seen in Figure 5, in which the letters A to H indicate the printing and post-treatment conditions that the parts were subjected to, as previously explained in Table 1. It is noticeable that the specimens submitted to the annealing process absorbed a much higher energy when compared to the other non-annealed specimens, with an increase of around 300%. This is also confirmed in the Pareto chart of effects of Figure 6, resultant from analysis of variance. This result may be associated with the fact that during annealing, which maintains the parts at a temperature above the T_g of the polymer, the greater mobility of the macromolecules allows for better intertwining of the polymer chains, improving adhesion between the deposited filaments (Seppala et al, 2017). Another possibility is the change suffered in the empty spaces configuration, which can coalesce and form structures of lower stress concentration, or even facilitate contact between the layers, as observed by Hart et al (2017). Another possibility of increasing the mechanical properties comes from the crystallization process itself, since the crystals act as barriers to the stretching of the amorphous chains, which is the initial mechanism of the elastoplastic deformation observed in thermoplastic polymers (Callister, 2006). It is also noticeable that the samples from D4508 had a slightly increased energy absorption when compared with D256, as shown in Figure 5 and confirmed in Figure 6, which may be due to the fact that the D256 samples had a chip that facilitates its fracture, while D4508 didn't have it.

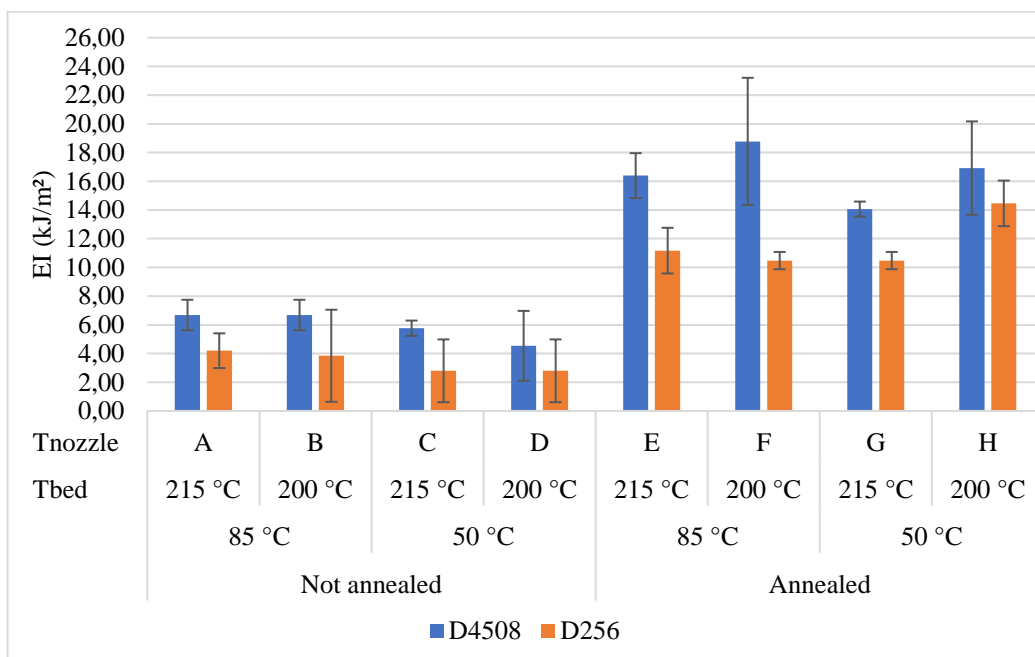


Figure 5. Graphic of the energy absorption by the samples of different standards.

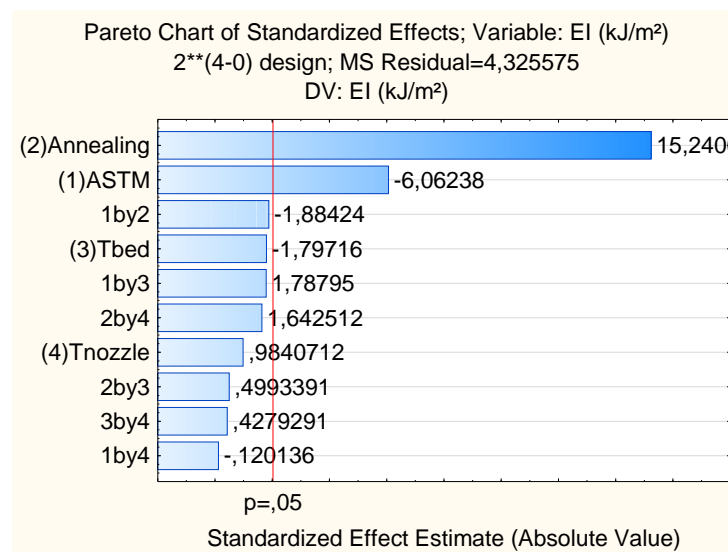


Figure 6. Pareto chart showing the most significant variables that affect the impact resistance of PLA printed parts.

The translucency of both the D256 and D4508 samples were also analyzed. Considering the standard deviations of the results, there wasn't much difference due to the sample geometries of different standards, but there was a slight increase in the average translucency of the annealed specimens, as seen in Figure 7. However, no variable was statistically significant in ANOVA. It is possible that all samples were too thin to cause a significant alteration of translucency, or that the time and temperature chosen for annealing did not affect the crystallization of the polymer so much.

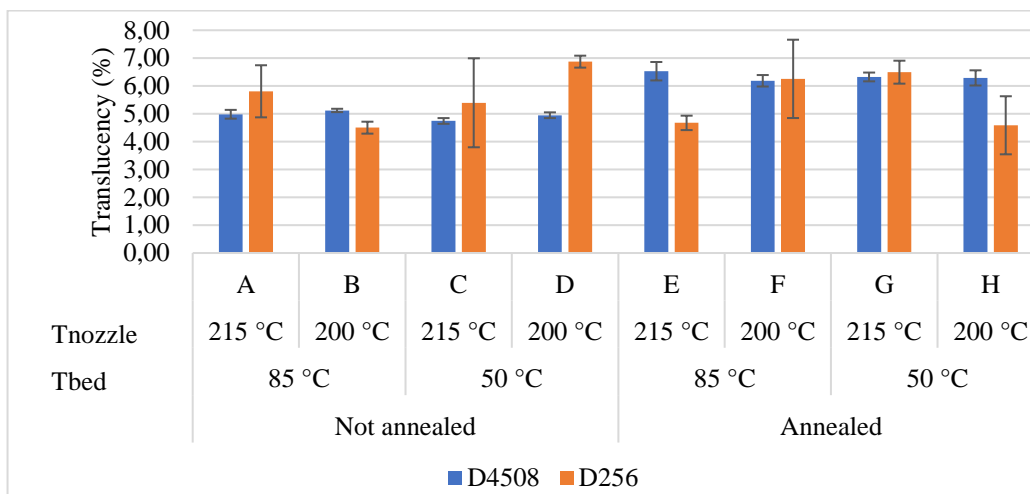


Figure 7. Graphic of the translucency for all samples.

Figure 8 shows the variations of length, width, and thickness of ASTM D256 samples. Although the results for the same sample production parameters vary greatly, as indicated by the large standard deviations, in average, there were some consistent variations. For instance, the table temperature of 85 °C and nozzle temperature of 200 °C of samples B and F caused samples to increase in length and thickness after annealing, while all other printing conditions caused the samples to shrink after annealed. It is important to highlight that the printing parameters can change the geometry of voids in the parts and affect crystal growth orientation. Although there is not a readily visible pattern to explain while only B samples increased in geometry after annealing, it could be associated with less voids between deposited filaments in this conditions, which could be a combination of better layer adhesion and more consistent filament deposition.

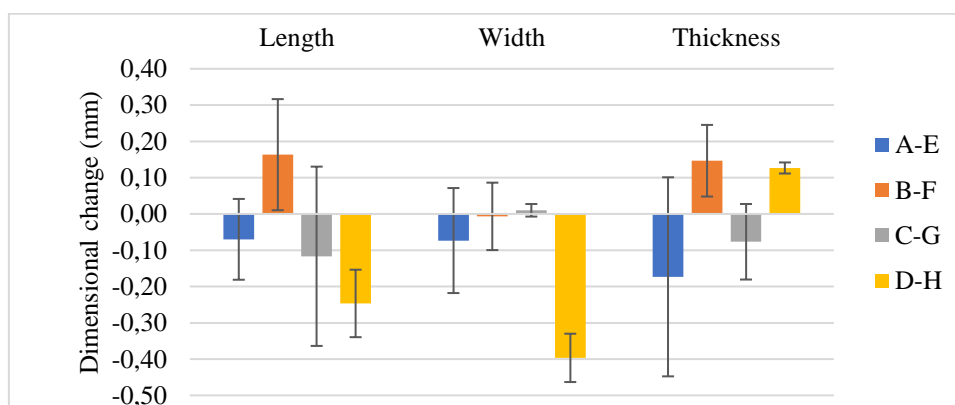


Figure 8. Graphic of the dimensional variation of the samples from ASTM D256.

4. CONCLUSION

With the greater accessibility to Fused Filament Fabrication processes, its use in research and applications in the industry becomes more common, making it important to evaluate simple and low-cost conditions that improve the resistance of the final parts. In this case, an average improvement of 300% on the Izod impact resistance was found when annealing the parts, both for ASTM D256 and D4508 standards. Although this could be explained both by change in the crystallinity of the parts and by better filament adhesion, it is likely that only the second has taken place, since there was no statistically significant change in the translucency of the samples with any of the variables, considering this factor is intimately correlated with polymer crystallinity. Overall, these results demonstrate a good efficiency of the annealing

technique, and by enabling the fine tuning of the printing parameters they constitute a simple and cheap way to improve the mechanical properties of the parts. It is important to highlight that although this kind of experiments allow optimization of the printing conditions, this was not carried in this work.

It is interesting to notice that the type of standard used was a significant parameter in the impact resistance. It is likely that the fact that the D256 samples had a chip on its side was the only cause for difference, since due to this all these samples will need less energy for the fracture to nucleate and propagate along the polymeric material. Another interesting point was the verification of geometric deviations due to the annealing process. This phenomenon is well reported in the literature and may occur due to filling of the voids left between deposited strands in printed parts, or due to crystallization which also changes the material density and specific volume. Since the translucency was not greatly affected as commented before, it is likely that only the first factor explains the overall trend of reducing the parts dimensions. Intriguingly, for one of the printing conditions, with higher table temperature and lower nozzle temperature, samples increased in length and thickness after annealing, on average, which could be related to smaller void volume during printing at these conditions.

5. ACKNOWLEDGEMENTS

The authors thank the CNPq, CAPES, FAPEMIG and DIRPE-UFU agencies for the financial support in the form of undergraduate and graduate scholarships.

6. REFERENCES

- Almeida, K. F., Veiga-Oliveira, P. H., Santos, T. O., da Silva, P. A. S., Borges, L. O. and Mariano, R. R. (2023). “Análise dos efeitos do recozimento na resistência ao impacto de peças poliméricas impressas por FFF”. Proceedings of the 12^o Brazilian Congress on Manufacturing Engineering -COBEF2023, Brasília.
- ASTM D256 (2018). Standard Test Methods for Determining the Izod Pendulum Impact Resistance of Plastics.
- ASTM D4508 (2006). Standard Test Method for Chip Impact Strength of Plastics.
- Aliheidari, N., Tripuraneni, R., Ameli, A., & Nadimpalli, S.,2017. Fracture resistance measurement of fused deposition modeling 3D printed polymers. *Polymer Testing*, 60, 94-101.
- Bhandari, S., Lopez-Anido, R. A., & Gardner, D. J.,2019. Enhancing the interlayer tensile strength of 3D printed short carbon fiber reinforced PETG and PLA composites via annealing. *Additive Manufacturing*, 30, 100922.
- Callister, W. D.,2006. Fundamentos da ciência e engenharia de materiais: uma abordagem integrada. *Editora LTC. Rio de Janeiro*.
- Gao, X., Qi, S., Kuang, X., Su, Y., Li, J., & Wang, D.,2021. Fused filament fabrication of polymer materials: A review of interlayer bond. *Additive Manufacturing*, 37, 101658.
- Hart, K. R., & Wetzel, E. D.,2017. Fracture behavior of additively manufactured acrylonitrile butadiene styrene (ABS) materials. *Engineering Fracture Mechanics*, 177, 1-13.
- Instrumentation Tools. Encoder Working Principle. <https://instrumentationtools.com/encoderworking-principle>.
- Lluch-Cerezo, J., Meseguer, M. D., García-Manrique, J. A., & Benavente, R. (2022). Influence of thermal annealing temperatures on powder mould effectiveness to avoid deformations in ABS and PLA 3D-printed parts. *Polymers*, 14(13), 2607.
- MatWeb. Izod Impact Strength Testing of Plastics. <https://www.matweb.com/reference/izodimpact.aspx>.
- Piorkowska, E., & Rutledge, G. C.,2013. (Eds.). Handbook of polymer crystallization. John Wiley & Sons.
- Seppala, J. E., Han, S. H., Hillgartner, K. E., Davis, C. S., & Migler, K. B.,2017. Weld formation during material extrusion additive manufacturing. *Soft matter*, 13(38), 6761-6769.
- Sood, A. K., Ohdar, R. K., & Mahapatra, S. S.,2010. Parametric appraisal of mechanical property of fused deposition modelling processed parts. *Materials & Design*, 31(1), 287-295.
- Sun, Q., Rizvi, G. M., Bellehumeur, C. T., & Gu, P.,2008. Effect of processing conditions on the bonding quality of FDM polymer filaments. *Rapid prototyping journal*.
- Torres, J., Cole, M., Owji, A., DeMastry, Z., & Gordon, A. P.,2016. An approach for mechanical property optimization of fused deposition modeling with polylactic acid via design of experiments. *Rapid Prototyping Journal*.
- Vaes, D., & Van Puyvelde, P.,2021. Semi-crystalline feedstock for filament-based 3D printing of polymers. *Progress in Polymer Science*, 101411.

7. RESPONSIBILITY NOTICE

The author(s) is (are) the only responsible for the printed material included in this paper.